

Floquet engineering of multi-orbital Mott insulators: applications to orthorhombic titanates

Jianpeng Liu,¹ Kasra Hejazi,² and Leon Balents¹

¹*Kavli Institute for Theoretical Physics, University of California, Santa Barbara CA 93106, USA*

²*Department of Physics, University of California, Santa Barbara CA 93106, USA*

We consider driving multi-orbital Mott insulators using laser radiation. We derive general expressions for periodically driven spin-orbital models using time-dependent perturbation theory in the strong interaction limit. We show that the effective exchange interactions of the Floquet spin-orbital Hamiltonian are highly tunable via variations of the frequency, amplitude, and polarization of the laser. We also take the effect of finite bandwidth of excitations into account and study possible heating effects. We further apply our formalism to orthorhombic titanates YTiO_3 and LaTiO_3 based on first-principles calculations, and find that the spin exchange interactions in these compounds can be engineered to a large extent by tuning the frequency and electric-field amplitude of the laser.

Periodically driven quantum systems have received significant attention in recent years. The typical theoretical prescription is to use the Floquet formalism [1, 2], which allows for the description of a time-periodic system using some effectively time-independent Hamiltonian dubbed as the “Floquet Hamiltonian”, $H_F = i\hbar \log U(T, 0)/T$, where $U(T, 0)$ is the time-evolution operator from time 0 to a full period T [3]. Despite the problem of thermalization at long times [4, 5], it has been argued that at experimentally accessible finite time scales the time evolution of the system is well described by the time-independent Floquet Hamiltonian [6].

Since the details of the Floquet Hamiltonian are crucially dependent on the frequency, amplitude and polarization of the external drive, the physical properties of a quantum system may be engineered using laser radiation. Such “Floquet engineering” has been extensively studied in the context of both single-particle [7–17] and many-body [18–29] models.

Here, we contemplate applications to the solid state, i.e. Mott insulating transition metal oxides, for which the orbital degrees of freedom plays an essential role [30–32]. We use many-body time-dependent perturbation theory to derive general expressions for effective spin-orbital model descriptions of multi-orbital Mott insulators in the presence of laser irradiation. We further include the effects of the doublon-holon (DH) hopping, i.e. the bandwidth of excitations, into account in our perturbation theory [33], which induces both real and imaginary parts into the effective Floquet Hamiltonian projected onto the spin-orbital subspace. The real part is interpreted as an effective spin-orbital model, and the corresponding exchange interactions are renormalized by the periodic driving, which allows for the Floquet engineering of the spin-orbital states. The imaginary part on the other hand is related to the rate of generation of DH pairs, and thus can capture the effects of heating. We further apply our formalism to ferromagnetic YTiO_3 and antiferromagnetic LaTiO_3 based on first-principles calculations. We find that the antiferromagnetic and fer-

romagnetic Mott insulators exhibit distinct responses to the laser radiation, and the exchange interactions in these compounds can be engineered to a large extent by moderate electric fields.

Floquet spin model: We start the discussion by reviewing the periodically driven Hubbard model:

$$H(t) = - \sum_{\langle ij \rangle \sigma} \left(t_h e^{i u_{ij} \sin \omega t} c_{i\sigma}^\dagger c_{j\sigma} + \text{h.c.} \right) + U \sum_i \hat{n}_{i\uparrow} \hat{n}_{i\downarrow}, \quad (1)$$

where t_h is the hopping amplitude between sites i and j , and $U \gg t_h$ is the onsite Coulomb repulsion energy. $u_{ij} = e \mathbf{E}_0 \cdot \mathbf{r}_{ij} / \omega$, where $|\mathbf{E}_0|$ denotes the magnitude of the AC electric field with frequency ω , $\mathbf{E}(t) = \mathbf{E}_0 \cos \omega t$, and $\mathbf{r}_{ij} = \mathbf{r}_j - \mathbf{r}_i$ is the displacement vector from lattice site i to j . The effective Floquet spin Hamiltonian in such a periodically driven half-filled Hubbard model has been extensively discussed in Ref. 25, 28, and 34. It has been shown that the effective spin exchange interaction of the Floquet spin Hamiltonian associated with the bond $\langle ij \rangle$ is renormalized due to the periodic driving, and becomes dependent on both the frequency and amplitude of the drive, $J_{\langle ij \rangle} = \sum_{n=-\infty}^{\infty} 4t_h^2 \mathcal{J}_n^2(u_{ij}) / (U - n\omega)$, which includes contributions from all the virtual DH excitation processes which absorb/emit n photons weighted by $\mathcal{J}_n^2(u_{ij})$, where $\mathcal{J}_n(u_{ij})$ is the n th Bessel function of the first kind. The energy of the virtually created DH pair which absorbs/emits n photons is just $U - n\omega$ if the effects of DH hopping are neglected.

The Floquet spin model breaks down when the photon energy ω (setting $\hbar=1$) is in resonance with the interaction energy U , i.e. $n\omega$ is around U . In such a resonance regime, the periodic driving generates real DH pairs, and the description of the system by the low-energy spin dynamics is no longer valid. The DH excitation spectrum has a finite bandwidth $\sim 4\sqrt{z-1}t_h$ (z is the coordination number) due to hopping of the DH pairs. As a result of this, real DH pairs are generated as long as the frequency $n\omega$ ($n \sim \mathcal{O}(1)$) is within this excitation band. On the contrary, when $n\omega$ is outside the DH band, the DH creation rate is tiny and the description of the system by

an effective Floquet spin Hamiltonian is still valid, but the expression for $J_{\langle ij \rangle}$ is modified by the DH hopping.

Following Ref. 33, a generic many-body state $|\Psi\rangle_t$ can be approximately expressed as $|\Psi\rangle_t \approx |\Psi_0\rangle_t + |\Psi_1\rangle_t$, where $|\Psi_n\rangle_t$ represents a state with n doubly occupied sites (doublons), and the $n > 1$ states have been neglected as they make higher order contributions to the spin dynamics. The Schrödinger equation for the evolution of the two components of the state reads

$$\begin{aligned} i\partial_t |\Psi_0\rangle_t &= \hat{P}_0 T_t |\Psi_1\rangle_t, \\ i\partial_t |\Psi_1\rangle_t &= U |\Psi_1\rangle_t + T_t |\Psi_0\rangle_t + \tilde{T}_t |\Psi_1\rangle_t, \end{aligned} \quad (2)$$

where T_t is the time-dependent hopping operator shown in Eq. (1), \hat{P}_n is the projector onto the subspace with n double occupancies, and $\tilde{T}_t = \hat{P}_1 T_t \hat{P}_1$ is the hopping operator projected onto the single-doublon space. Replacing \tilde{T}_t by its time average $\bar{T} = (\omega/2\pi) \int_0^{2\pi/\omega} dt' \tilde{T}_{t'}$, $|\Psi_1\rangle_t$ can be explicitly expressed as a function of $|\Psi_0\rangle_t$ [33]. Plugging the expression of $|\Psi_1\rangle_t$ (in terms of $|\Psi_0\rangle_t$) back into the first line of Eq. (2), one would obtain the time-dependent Schrödinger equation projected onto the $|\Psi_0\rangle$ subspace. If we further assume that the dominant DH hopping processes are those which create and annihilate the DH pairs at the same lattices sites leaving the background spin configurations unchanged, then it follows that [33]

$$i\partial_t |\Psi_0\rangle_t = \sum_{\langle ij \rangle} \sum_{m,n=-\infty}^{\infty} H_{ij}^{mn}(t) |\Psi_0\rangle_t, \quad (3)$$

where $H_{ij}^{mn}(t) = t_h^2 f_{jij}^{mn}(t) \sum_{\sigma\sigma'} c_{j\sigma'}^\dagger c_{i\sigma'} c_{i\sigma}^\dagger c_{j\sigma} g_{dh}(n\omega)$, and $g_{dh}(n\omega) = \langle \Psi_0 | c_{j\sigma}^\dagger c_{i\sigma} (U - n\omega + \bar{T})^{-1} c_{i\sigma}^\dagger c_{j\sigma} | \Psi_0 \rangle$ is the DH Green's function, and $f_{jij}^{mn}(t) = -e^{i(m-n)\omega t} \mathcal{J}_{-n}(u_{ij}) \mathcal{J}_m(u_{ji})$. We further assume that the motions of the doublons and holons are uncorrelated, which allows g_{dh} to be expressed as the convolution of the holon and doublon Green's functions g_d and g_h [33]. The holon (doublon) Green's function $g_{h(d)}$ is then calculated using the retraceable path approximation $g_{h(d)}(E) = 2(z-1)/(E(z-2) + z\sqrt{E^2 - 4(z-1)\bar{t}_h^2})$ [33, 35], where $\bar{t}_h = t_h \mathcal{J}_0(u_{ij})$ denotes the time-averaged hopping amplitude. In the regime $\omega \gg t_h^2/U$, the leading order Floquet Hamiltonian is simply the time-average of the right-hand-side of Eq. (3).

Floquet spin-orbital model: The previous discussion of the periodically driven Hubbard model can be generalized to the case of multi-orbital Mott insulators with local Kanamori interactions [36]

$$\begin{aligned} H_K = & U \sum_{i,\alpha} \hat{n}_{i\alpha\uparrow} \hat{n}_{i\alpha\downarrow} + U' \sum_{i,\alpha<\beta,\sigma,\sigma'} \hat{n}_{i\alpha\sigma} \hat{n}_{i\beta\sigma'} \\ & - J_H \sum_{i,\alpha<\beta,\sigma,\sigma'} c_{i\alpha\sigma}^\dagger c_{i\alpha\sigma'} c_{i\beta\sigma'}^\dagger c_{i\beta\sigma} \\ & + J_P \sum_{i,\alpha<\beta,\sigma} c_{i\alpha\sigma}^\dagger c_{i\alpha-\sigma}^\dagger c_{i\beta\sigma} c_{i\beta-\sigma}, \end{aligned} \quad (4)$$

where U and U' are the intra-orbital and inter-orbital direct Coulomb interactions. J_H and J_P denote the Hunds' coupling and pair hoppings respectively; the sets of indices $\{i, j\}$, $\{\alpha, \beta\}$, $\{\sigma, \sigma'\}$ denote, in turn, the lattice sites, orbitals and spin degrees of freedom. As in the case of the Hubbard model, the effect of the periodic driving is manifested in the kinetic energy via the Peierls substitution,

$$T_t = \sum_{\langle ij \rangle, \alpha, \beta, \sigma} \left(t_{i\alpha, j\beta} e^{iu_{ij} \sin \omega t} c_{i\alpha\sigma}^\dagger c_{j\beta\sigma} + \text{h.c.} \right), \quad (5)$$

where $t_{i\alpha, j\beta}$ represents the hopping amplitude from orbital β at site j to orbital α at site i .

In the multi-orbital case, we also need to consider the crystal-field splittings (H_{CF}). In addition to the giant $t_{2g} - e_g$ splitting of typical perovskite transition-metal oxides, there may be additional splittings within the t_{2g} and/or e_g manifold due to various distortions [32, 37]. Throughout this paper we only consider the t_{2g} orbitals. Within the quasi-degenerate t_{2g} levels we further include the crystal-field splittings,

$$H_{CF} = \sum_i \sum_{\alpha, \beta, \sigma} \epsilon_{i, \alpha, \beta} c_{i\alpha\sigma}^\dagger c_{i\beta\sigma}, \quad (6)$$

Including all these terms, we find the total periodically driven Hamiltonian as $H_t = T_t + H_K + H_{CF}$ [52]

We consider the limit that the typical interaction energy scale is much greater than the hopping energy scale and consider T_t as a perturbation to H_K . In the non-driven case, the low-energy physics is dominated by the spin and orbital dynamics, which is well described by the Kugel-Khomskii [32, 38] and similar spin-orbital models, and can be derived using second-order perturbation theory. We generalize that approach to the case with periodic driving, and derive a time-dependent spin-orbital model using time-dependent perturbation theory. We consider the situation of one occupied electron at every site in the ground state of the static system, then make the assumption that $U' = U - J_H$ and $J_P = 0$ [31]. With such an assumption H_K is rotationally invariant and there are only two distinct multiplet energy levels: $E_{\text{singlet}} = U$, for spin singlets, and $E_{\text{triplet}} = U - 2J_H$ for spin triplets [31]. Therefore, we expand an arbitrary many-body state $|\Psi\rangle_t$ as $|\Psi\rangle_t \approx |\Psi_0\rangle_t + |\Psi_1^s\rangle_t + |\Psi_1^t\rangle_t$, where $|\Psi_0\rangle_t$ represents the states without any double occupancy, and $|\Psi_1^s\rangle$ and $|\Psi_1^t\rangle$ denote the single-doublon states with spin singlets and triplets configurations. As discussed above, we neglect the excited states with more than one doublons.

Time-dependent perturbation theory leads to the Schrödinger equation projected onto the zero-doublon subspace [33],

$$i\partial_t |\Psi_0\rangle_t = \left(\sum_{\langle ij \rangle, mn, a} f_{ij}^{mn}(t) \hat{G}_{jij}^a(n\omega) + H_{CF} \right) |\Psi_0\rangle_t, \quad (7)$$

where $f_{ij}^{mn}(t) = -e^{i(m-n)\omega t} \mathcal{J}_m(u_{ji}) \mathcal{J}_{-n}(u_{ij})$, $\hat{G}_{jij}^a = \sum_{\alpha\beta\alpha'\beta',\sigma\sigma'} t_{i\alpha,j\beta} t_{j\beta',i\alpha'} c_{j\beta'\sigma'}^\dagger c_{i\alpha'\sigma'} c_{i\alpha\sigma}^\dagger c_{j\beta\sigma} g_{dh}^a$, and the superscript index “a” runs over {s, t}. g_{dh}^s and g_{dh}^t are the doublon-holon Green’s functions in the spin singlet and triplet configurations:

$$g_{dh}^s = \langle \Psi_0 | c_{j\beta\sigma}^\dagger c_{i\alpha\sigma} \frac{\hat{P}_{1s}}{U - n\omega + \bar{T}_{ss}} c_{i\alpha\sigma}^\dagger c_{j\beta\sigma} | \Psi_0 \rangle, \\ g_{dh}^t = \langle \Psi_0 | c_{j\beta\sigma}^\dagger c_{i\alpha\sigma} \frac{\hat{P}_{1t}}{U - 2J_H - n\omega + \bar{T}_{tt}} c_{i\alpha\sigma}^\dagger c_{j\beta\sigma} | \Psi_0 \rangle. \quad (8)$$

We have made the following approximations in deriving Eq. (7)-(8). First, we only consider the hopping processes which create and annihilate DH pairs at the same sites, with a final *spin-orbital* configuration which is identical to the initial configuration. Second we have neglected the doublon-holon hopping terms which convert a spin triplet to a singlet and vice versa. Lastly, we have time-averaged over the hopping operator projected onto the single doublon-holon space [33].

In order to calculate the holon/doublon Green’s function g_h/g_h in the multi-orbital case, we take the limit that the crystal field splitting (within the t_{2g} or e_g orbitals) is much larger than the intersite exchange energy, such that the occupied orbital at site i is uniquely determined and is denoted as $|1\rangle_i$. In this classical-orbital regime, it is legitimate to introduce effective hoppings between the orbitals $|1\rangle_i$ and $|1\rangle_j$ for the singlet and triplet virtual excitations denoted as $t_{i1,j1}^s$ and $t_{i1,j1}^t$: $(t_{i1,j1}^s)^2 = \sum_{\alpha} (|t_{i1,j\alpha}|^2 + |t_{j1,i\alpha}|^2)/2$, and $(t_{i1,j1}^t)^2 = \sum_{\alpha \neq 1} (|t_{i1,j\alpha}|^2 + |t_{j1,i\alpha}|^2)/2$. Then the corresponding DH Green’s functions g_{dh}^s and g_{dh}^t can be calculated using the single-orbital formalism discussed above.

When ω is much larger than typical exchange energies, the leading-order Floquet spin-orbital Hamiltonian is simply the time-average of the right-hand-side of Eq. (7). For t_{2g} orbitals the Floquet Hamiltonian can be rewritten in terms of the t_{2g} spin and orbital operators. After taking the expectation values of the orbital operators, one obtains

$$H_F^{so} = \sum_{\langle ij \rangle, n} \left(\mathcal{J}_n^2(u_{ij})(\gamma_1 + \gamma_2) g_{dh}^s(n\omega) (\mathbf{S}_i \cdot \mathbf{S}_j - \frac{1}{4}) \right. \\ \left. - \mathcal{J}_n^2(u_{ij})(\gamma_1 - \gamma_2) g_{dh}^t(n\omega) (\mathbf{S}_i \cdot \mathbf{S}_j + \frac{3}{4}) \right). \quad (9)$$

It follows that the effective spin exchange interaction associated with bond $\langle ij \rangle$ is

$$\bar{J}_{ij} = \sum_n \mathcal{J}_n^2(u_{ij}) ((\gamma_1 + \gamma_2) g_{dh}^s - (\gamma_1 - \gamma_2) g_{dh}^t). \quad (10)$$

where $\gamma_1 = \sum_{\alpha,\beta,\beta'=1}^3 (t_{i\alpha,j\beta} t_{j\beta',i\alpha} \langle \hat{A}_{\beta'\beta}^j \rangle + i \leftrightarrow j)$, and $\gamma_2 = \sum_{\alpha,\alpha',\beta,\beta'=1}^3 (t_{i\alpha,j\beta} t_{j\beta',i\alpha'} \langle \hat{A}_{\beta'\beta}^j \rangle \langle \hat{A}_{\alpha\alpha'}^i \rangle + i \leftrightarrow j)$ and $\langle \hat{A}_{\alpha\alpha'}^i \rangle = \sum_{\sigma} \langle c_{i\alpha\sigma}^\dagger c_{i\alpha'\sigma} \rangle$ is the expectation value of

the orbital operator $\hat{A}_{\alpha\alpha'}^i$. The DH Green’s function in the singlet (triplet) configuration $g_{dh}^{s(t)}$ can be calculated using the single-orbital formalism in the regime of strong crystal-field splittings.

As in the case of non-driven system, the Floquet exchange interaction \bar{J}_{ij} consists of two components: the antiferromagnetic component from all the singlet virtual excitations $\bar{J}_{ij}^{\text{AFM}} = \sum_n \mathcal{J}_n^2(u_{ij})(\gamma_2 + \gamma_1) g_{dh}^s$, and the ferromagnetic component from all the triplet virtual excitations $\bar{J}_{ij}^{\text{FM}} = -\sum_n \mathcal{J}_n^2(u_{ij})(\gamma_1 - \gamma_2) g_{dh}^t$. Eq. (10) suggests that the effective exchange interactions in periodically driven multiorbital Mott insulators can be engineered by the periodic driving.

If the $|U - n\omega|$ and/or $|U - 2J_H - n\omega|$ [39] is much greater than the typical hopping amplitudes, it is straightforward to show that $g_{dh}^s(n\omega) \approx 1/(U - n\omega)$ and $g_{dh}^t(n\omega) \approx 1/(U - 2J_H - n\omega)$. Eq. (10) becomes

$$\bar{J}_{ij} = \sum_n \mathcal{J}_n^2(u_{ij}) \left(\frac{\gamma_1 + \gamma_2}{U - n\omega} - \frac{\gamma_1 - \gamma_2}{U - 2J_H - n\omega} \right). \quad (11)$$

In what follows we will show that ferromagnetic and antiferromagnetic Mott insulators exhibit contrasting responses to laser radiation due to the analytic structure of \bar{J}_{ij} shown in Eq. (11). On the other hand, if $|U - n\omega| < 4\sqrt{z - 1}t_h$ or $|U - 2J_H - n\omega| < 4\sqrt{z - 1}t_h$, g_{dh}^s or g_{dh}^t has both real and imaginary parts. The non-vanishing imaginary part of the Floquet spin-orbital Hamiltonian ($\text{Im}[H_F^{so}]$) implies the norm of the spin-orbital state $|\Psi_0\rangle$ decays with time, and the rate of the DH generation is proportional to $\text{Im}[H_F^{so}]$.

Application to orthorhombic titanates: We apply the formalism discussed above to the orthorhombic perovskite titanates YTiO_3 and LaTiO_3 . YTiO_3 is a ferromagnet Mott insulator with Curie temperature $T_C \approx 27$ K [40], whereas LaTiO_3 is a “G-type” antiferromagnetic Mott insulator (antiferromagnetic ordering in all the three spatial dimensions) with Neel temperature $T_N \approx 146$ K [41]. Both compounds can be considered as perovskite oxides with GdFeO_3 -type distortions. Moreover, there are other lattice distortions which split the otherwise degenerate t_{2g} orbitals [42]. The crystal field splittings $\sim 0.1 - 0.4$ eV [43–45], are much larger than the exchange energies. Hereafter we assume that the orbital patterns are completely fixed by the crystal field splittings and neglect orbital fluctuations.

In order to evaluate the hopping parameters (Eq. (5)) and the crystal-field splittings H_{CF} , we carried out bare density-functional-theory (DFT)[46, 47] calculations with vanishing magnetizations for LaTiO_3 and YTiO_3 . The converged Bloch functions are then projected onto the local t_{2g} orbitals at the Ti sites to generate Wannier functions with the t_{2g} symmetry. Realistic tight-binding models are then constructed in the basis of the t_{2g} Wannier functions [48, 49]. From these tight-binding models we extract the hopping parameters

and the crystal-field parameters [42]. We have also estimated the Hubbard repulsion using the linear-response method [50]. We find that $U = 3.83$ eV, $J_H = 0.64$ eV in YTiO₃; while $U = 3.82$ eV and $J_H = 0.64$ eV for LaTiO₃. Using these parameters, the nearest-neighbor spin exchange within the ab plane $J_{ab} = -8.4$ meV (minus sign means ferromagnetic), and $J_c = -0.5$ meV along the c axis for YTiO₃. We note that the in-plane (inter-plane) ferromagnetic exchange interaction of YTiO₃ is overestimated (underestimated) by DFT. On the other hand, for LaTiO₃ we get antiferromagnetic exchange interactions with $J_{ab} = 15.4$ meV and $J_c = 11.9$ meV, which are in good agreements with the spin-wave measurements [51].

First we consider the Floquet exchange interactions neglecting the bandwidth of the DH excitations as given by Eq. (11). Plugging all the hopping, crystal-field, and interaction parameters evaluated from DFT into Eq. (11), the effective spin exchange interaction for the bond $\langle ij \rangle$ can be readily obtained. Neglecting the bandwidth of the DH excitations, in Fig. 1(a)-(b) we plot the in-plane effective spin exchange interactions for YTiO₃ (Fig. 1(a)) and LaTiO₃ (Fig. 1(b)) in the parameter space (ω, V_{ij}) , where $V_{ij} = u_{ij}\omega$ is the electric-field energy.

We notice that at relatively low frequencies and weak electric fields, i.e. $u_{ij} \lesssim 1$, $\omega \ll U, U - 2J_H$, the effective ferromagnetic exchange interaction in YTiO₃ is enhanced, but the antiferromagnetic exchange in LaTiO₃ is suppressed as V_{ij} increases. Such opposite behaviors are inherited from the analytic structure of Eq. (11). When u_{ij} is small and $\omega \ll U, U - 2J_H$, the dominant processes are those with a small number of photon emissions/absorptions since the weight $\mathcal{J}_n^2(u_{ij}) \sim u_{ij}^{2n}$ for small u_{ij} . Up to second order in u_{ij} , the effective spin exchange interaction (neglecting the effects of the virtual DH hopping) for bond $\langle ij \rangle$ simplifies to $\bar{J}_{\langle ij \rangle} \approx (\gamma_2 + \gamma_1)(1/U + \delta J_U) - (\gamma_1 - \gamma_2)(1/(U - 2J_H) + \delta J_{U-2J_H})$, where δJ_E (with $E = U, U - 2J_H$) is understood as the corrections to the exchange interaction in the static limit, $2\delta J_E = u_{ij}^2 E (1/(E^2 - \omega^2) - 1/E^2)$. We note that δJ_E is always positive, and $\delta J_{U-2J_H} > \delta J_U$ for small ω . As a result, when the total exchange is ferromagnetic (antiferromagnetic) in the static limit, the magnitude of the exchange is enhanced (diminished) as V_{ij} increases.

More interesting behavior appears when the frequency is on the same order of magnitude as U and is in between two virtual excitation levels. To be specific, if $(U - 2J_H)/n_2 < \omega < U/n_1$ ($n_1, n_2 \sim 1$), it is convenient to express the photon energy as $\omega = (U - 2J_H)/n_2 + \delta\omega_2 = U/n_1 - \delta\omega_1$. It follows that the dominant photon absorption/emission processes are those with $n=0$, n_1 and n_2 , and the effective Floquet exchange interaction associated with bond $\langle ij \rangle$ is approximated as $J_{\langle ij \rangle} \approx \mathcal{J}_0^2(u_{ij})((\gamma_2 + \gamma_1)/U - (\gamma_1 - \gamma_2)/(U - 2J_H)) + \delta J_{\langle ij \rangle}^{n_1} + \delta J_{\langle ij \rangle}^{n_2}$, where $\delta J_{\langle ij \rangle}^{n_1} = \mathcal{J}_{n_1}^2(u_{ij})((\gamma_2 + \gamma_1)/(n_1\delta\omega_1) + (\gamma_1 - \gamma_2)/(2J_H - n_1\delta\omega_1))$, and $\delta J_{\langle ij \rangle}^{n_2} = \mathcal{J}_{n_2}^2(u_{ij})((\gamma_2 + \gamma_1)/(2J_H - n_2\delta\omega_2) +$

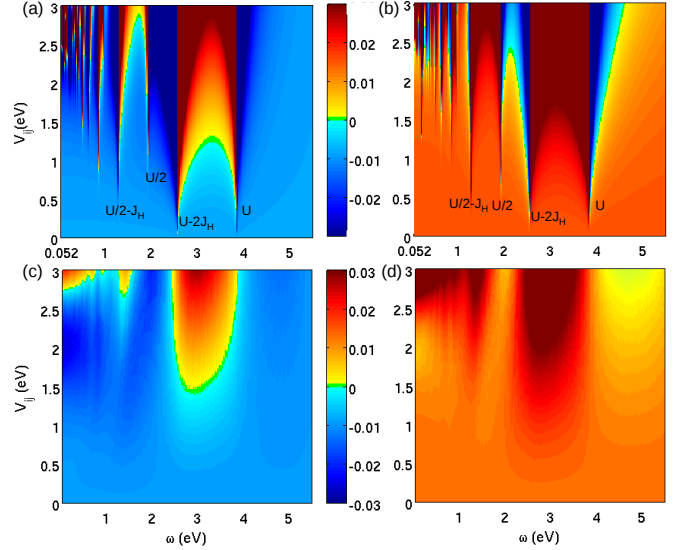


FIG. 1: The in-plane Floquet spin exchange interactions for YTiO₃ and LaTiO₃ as a function of the driving frequency ω and the electric-field energy V_{ij} . In (a)-(b), the bandwidth of the virtual doublon-holon excitations is neglected. In (c)-(d), the bandwidth of the virtual excitation spectra has been taken into account. (a) and (c) are for YTiO₃, and (b) and (d) are for LaTiO₃.

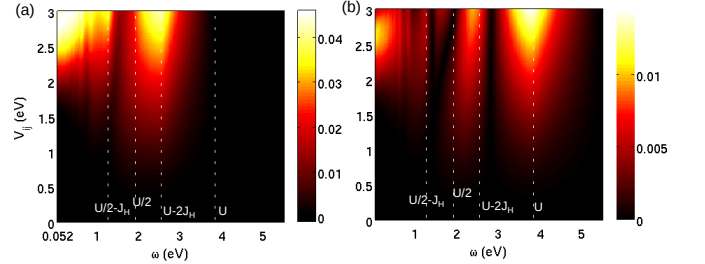


FIG. 2: The imaginary part of the Floquet spin-orbital Hamiltonian projected to the bond $\langle ij \rangle$, (a) for YTiO₃ and (b) LaTiO₃.

$(\gamma_1 - \gamma_2)/(n_2\delta\omega_2)$). We note that $\delta J_{\langle ij \rangle}^{n_1}$ and $\delta J_{\langle ij \rangle}^{n_2}$ are always positive, which would enhance the net antiferromagnetic exchange and suppress the net ferromagnetic exchange. This is clearly illustrated in Fig. 1(a)-(b) for $U - 2J_H < \omega < U$. For YTiO₃ (Fig. 1(a)), the ferromagnetic exchange at $V_{ij} = 0$ is suppressed by turning on the electric field, and becomes antiferromagnetic at some critical value of $V_{ij}^*(\omega) \sim 0.5 - 1.5$ eV. On the other hand, the antiferromagnetic exchange for LaTiO₃ in Fig. 1(b) is enhanced as V_{ij} increases. Similarly, if $U/n_1 < \omega < (U - 2J_H)/n_2$, it is straightforward to show that periodic driving tends to enhance the magnitude of the ferromagnetic exchange but suppress the antiferromagnetic exchange, as shown in Fig. 1(a)-(b) for $U/2 < \omega < U - 2J_H$.

Including the hopping within the DH subspace smears out the sharp patterns of the effective exchange interac-

tions shown in Fig. (1)(a)-(b), and introduces imaginary parts to the Floquet spin-orbital Hamiltonians when ω is in resonance with the excitation bands. In Fig. 1(c) and (d) we plot the real parts of the in-plane effective exchange interactions for YTiO_3 and LaTiO_3 , taking into account the bandwidth of the excitation spectra due to the DH hopping. The interesting features in Fig. 1(a)-(b) are mostly preserved in Fig. 1(c)-(d), except that the sign flip of the exchange interaction in LaTiO_3 (Fig. 1(c)) has been completely smeared out by DH hopping. We also plot the imaginary part of H_F^{so} (Eq. (9)) projected to the in-plane bond $\langle ij \rangle$ for both YTiO_3 ((a)) and LaTiO_3 ((b)). We have assumed that the spin order is ferromagnetic (antiferromagnetic) in YTiO_3 (LaTiO_3). Clearly $\text{Im}[H_F^{\text{so}}]$ has a broad peak centered at U ($U - 2J_H$) for the antiferromagnet (ferromagnet). Moreover in LaTiO_3 $\text{Im}[H_F^{\text{so}}]$ is significant between $U/2$ and $U - 2J_H$, which invalidates the description of the system by an effective spin(-orbital) Hamiltonian in this frequency regime.

To summarize, we have derived the Floquet spin-orbital model for multi-orbital Mott insulators using time-dependent perturbation theory, taking into account the effects of the bandwidth of the DH excitations. We have applied our formalism to orthorhombic perovskite titanates YTiO_3 and LaTiO_3 based on first-principles calculations. In certain frequency regimes the effective spin exchange interactions are highly tunable by the laser field, and exhibit robust features which may be experimentally measurable. The formalism and methodology presented in this paper can be directly applied to Slater/Mott insulators with any kind of ordered spin-orbital ground state, which may stimulate further exploration of Floquet engineering of magnetism in strongly correlated transition-metal oxides.

Acknowledgements: This research was supported by the NSF materials theory program through grant DMR1506119 (LB, KH) and the Army Research Office MURI grant ARO W911NF-16-1-0361, Floquet engineering and metastable states (JL).

[1] J. H. Shirley, Phys. Rev. **138**, B979 (1965).
[2] H. Sambe, Phys. Rev. A **7**, 2203 (1973).
[3] M. Bukov, L. D'Alessio, and A. Polkovnikov, Advances in Physics **64**, 139 (2015).
[4] L. D'Alessio and M. Rigol, Phys. Rev. X **4**, 041048 (2014).
[5] A. Lazarides, A. Das, and R. Moessner, Phys. Rev. E **90**, 012110 (2014).
[6] T. Kuwahara, T. Mori, and K. Saito, Annals of Physics **367**, 96 (2016).
[7] T. Oka and H. Aoki, Phys. Rev. B **79**, 081406 (2009).
[8] T. Kitagawa, T. Oka, A. Brataas, L. Fu, and E. Demler, Phys. Rev. B **84**, 235108 (2011).
[9] N. H. Lindner, G. Refael, and V. Galitski, Nature Physics **7**, 490 (2011).

[10] J.-i. Inoue and A. Tanaka, Phys. Rev. Lett. **105**, 017401 (2010).
[11] M. Ezawa, Phys. Rev. Lett. **110**, 026603 (2013).
[12] P. Delplace, A. Gómez-León, and G. Platero, Phys. Rev. B **88**, 245422 (2013).
[13] T. Kitagawa, E. Berg, M. Rudner, and E. Demler, Phys. Rev. B **82**, 235114 (2010).
[14] M. S. Rudner, N. H. Lindner, E. Berg, and M. Levin, Phys. Rev. X **3**, 031005 (2013).
[15] P. Titum, E. Berg, M. S. Rudner, G. Refael, and N. H. Lindner, Phys. Rev. X **6**, 021013 (2016).
[16] Y. Wang, H. Steinberg, P. Jarillo-Herrero, and N. Gedik, Science **342**, 453 (2013).
[17] F. Mahmood, C.-K. Chan, Z. Alpichshev, D. Gardner, Y. Lee, P. A. Lee, and N. Gedik, Nature Physics **12**, 306 (2016).
[18] D. Fausti, R. Tobey, N. Dean, S. Kaiser, A. Dienst, M. C. Hoffmann, S. Pyon, T. Takayama, H. Takagi, and A. Cavalleri, science **331**, 189 (2011).
[19] R. Mankowsky, A. Subedi, M. Först, S. Mariager, M. Chollet, H. Lemke, J. Robinson, J. Glowia, M. Minitti, A. Frano, et al., Nature **516**, 71 (2014).
[20] M. Mitrano, A. Cantaluppi, D. Nicoletti, S. Kaiser, A. Perucchi, S. Lupi, P. Di Pietro, D. Pontiroli, M. Riccò, S. R. Clark, et al., Nature **530**, 461 (2016).
[21] M. Knap, M. Babadi, G. Refael, I. Martin, and E. Demler, Phys. Rev. B **94**, 214504 (2016).
[22] M. Babadi, M. Knap, I. Martin, G. Refael, and E. Demler, arXiv preprint arXiv:1702.02531 (2017).
[23] A. Singer, S. K. K. Patel, R. Kukreja, V. Uhlí, J. Wingert, S. Festersen, D. Zhu, J. M. Glowia, H. T. Lemke, S. Nelson, et al., Phys. Rev. Lett. **117**, 056401 (2016).
[24] K. W. Kim, A. Pashkin, H. Schäfer, M. Beyer, M. Porer, T. Wolf, C. Bernhard, J. Demsar, R. Huber, and A. Leitenstorfer, Nature Materials **11**, 497 (2012).
[25] J. Mentink, K. Balzer, and M. Eckstein, Nature communications **6** (2015).
[26] J. Mentink, Journal of Physics: Condensed Matter **29**, 453001 (2017).
[27] K. Takasan, M. Nakagawa, and N. Kawakami, arXiv preprint arXiv:1706.06114 (2017).
[28] M. Claassen, H.-C. Jiang, B. Moritz, and T. P. Devereaux, arXiv preprint arXiv:1611.07964 (2016).
[29] A. G. Grushin, Á. Gómez-León, and T. Neupert, Physical review letters **112**, 156801 (2014).
[30] Y. Tokura and N. Nagaosa, science **288**, 462 (2000).
[31] A. Georges, L. de'Medici, and J. Mravlje, Annual Review of Condensed Matter Physics **4**, 137 (2013).
[32] K. I. Kugel and D. I. Khomskii, Sov. Phys. Usp **25**, 231 (1982).
[33] K. Hejazi, J. Liu, and L. Balents, manuscript to be submitted.
[34] M. Bukov, M. Kolodrubetz, and A. Polkovnikov, Phys. Rev. Lett. **116**, 125301 (2016).
[35] W. F. Brinkman and T. M. Rice, Phys. Rev. B **2**, 1324 (1970).
[36] J. Kanamori, Progress of Theoretical Physics **30**, 275 (1963).
[37] E. Pavarini, S. Biermann, A. Poteryaev, A. I. Lichtenstein, A. Georges, and O. K. Andersen, Phys. Rev. Lett. **92**, 176403 (2004).

- [38] K. I. Kugel and D. I. Khomskii, Zh. Eksp. Teor. Fiz **64**, 1429 (1973).
- [39] The important photon absorption/emission processes are dominated by those with n being on the order of unity. Because when n is large, the corresponding weight factor $\mathcal{J}_n(\mu_{ij})^2$ becomes negligible.
- [40] C. Ulrich, G. Khaliullin, S. Okamoto, M. Reehuis, A. Ivanov, H. He, Y. Taguchi, Y. Tokura, and B. Keimer, Phys. Rev. Lett. **89**, 167202 (2002).
- [41] M. Cwik, T. Lorenz, J. Baier, R. Müller, G. André, F. Bourée, F. Lichtenberg, A. Freimuth, R. Schmitz, E. Müller-Hartmann, et al., Phys. Rev. B **68**, 060401 (2003).
- [42] See Supplemental Information for the spin and orbital properties of YTiO₃ and LaTiO₃, the estimate of the AC Stark effect, as well as the details of the first principles calculations.
- [43] J. Akimitsu, H. Ichikawa, N. Eguchi, T. Miyano, M. Nishi, and K. Kakurai, Journal of the Physical Society of Japan **70**, 3475 (2001).
- [44] E. Pavarini, A. Yamasaki, J. Nuss, and O. Andersen, New Journal of Physics **7**, 188 (2005).
- [45] I. V. Solov'yev, Phys. Rev. B **69**, 134403 (2004).
- [46] P. Hohenberg and W. Kohn, Phys. Rev. **136**, B864 (1964).
- [47] W. Kohn and L. J. Sham, Phys. Rev. **140**, A1133 (1965).
- [48] N. Marzari, A. A. Mostofi, J. R. Yates, I. Souza, and D. Vanderbilt, Rev. Mod. Phys. **84**, 1419 (2012).
- [49] A. A. Mostofi, J. R. Yates, Y. S. Lee, I. Souza, D. Vanderbilt, and N. Marzari, Computer Phys. Comm. **178**, 685 (2008).
- [50] M. Cococcioni and S. de Gironcoli, Phys. Rev. B **71**, 035105 (2005).
- [51] B. Keimer, D. Casa, A. Ivanov, J. W. Lynn, M. v. Zimmermann, J. P. Hill, D. Gibbs, Y. Taguchi, and Y. Tokura, Phys. Rev. Lett. **85**, 3946 (2000).
- [52] The virtual excitations from the low-energy $3d$ levels to the high-energy $4p$ levels would induce further splittings of the $3d$ states via the second-order Stark effect, but such splittings are very small for $3d$ transition metal ions (see supplemental information).